ISOSCALAR DIPOLE RESPONSE IN ^{92}Mo AND ^{100}Mo ISOTOPES

RESPUESTA DIPOLAR ISOESCALAR EN LOS ISÓTOPOS ^{92}Mo Y ^{100}Mo

Gullala A. Mohammed, Ali H. Taqi*

Department of Physics, College of Science, Kirkuk University, Kirkuk, Iraq.

(Recibido: 03/2023. Aceptado: 06/2023)

Abstract

In this work, the Isoscalar (IS) Giant Dipole Resonance (GDR) and Pygmy Dipole Resonance (PDR) of ^{92}Mo and ^{100}Mo Isotopes were calculated in the farmwork of the self-consistent quasi-particle random phase approximation (QRPA) based on the results of Hartree-Fock-Bardeen, Cooper and Schrieffer (HF-BCS) using 10 Skyrme-type interactions: KDE0v1, eMSL08, SKX, SGOI, v080, SKP, SIV, SIII, SKIII, and SGI. The strength distributions of isoscalar dipole response were compared with the available experimental data. Also, we discussed the statistical relation between the centroid energy and the nuclear matter incompressibility K_{NM}.

Keywords: strength distribution; isoscalar dipole response; Skyrme force; Hartree-Fock-Bardeen-Cooper-Schrieffer; HF+BCS; quasiparticle random phase approximation; QRPA.

Resumen

En este trabajo se calcularon las resonancias dipolares gigantes (GDR) isoescalares y las resonancias dipolares pigmeas (PDR) de los isótopos ^{92}Mo y ^{100}Mo en el marco de la aproximación de fase aleatoria de cuasipartículas autoconsistente (QRPA) basada en los resultados de

* alitaqi@uokirkuk.edu.iq doi: https://doi.org./10.15446/mo.n67.107907

Hartree-Fock-Bardeen, Cooper y Schrieffer (HF-BCS) utilizando 10 interacciones de tipo Skyrme: KDE0v1, eMSL08, SKX, SGOI, v080, SKP, SIV, SIII, SKIII y SGI. Se compararon las distribuciones de fuerza de la respuesta dipolar isoescalar con los datos experimentales disponibles. Además, se discutió la relación estadística entre la energía del centroide y la incompresibilidad de la materia nuclear K_{NM}.

Palabras clave: distribución de fuerza; respuesta dipolar isoescalar; fuerza de Skyrme; Hartree-Fock-Bardeen-Cooper-Schrieffer; HF+BCS; aproximación de fase aleatoria de cuasipartículas; QRPA.

Introduction

There are many methods and theories developed to explain experimental observations of nuclear structure. These methods range from direct solutions and conjecture to more sophisticated models: ab initio calculation based on bare N-N interaction [1, 2] for (nuclei with mass number $A < 50$) a shell model Monte Carlo Methods [3, 4] for (nuclei with mass number $A > 60$), relativistic [5] and nonrelativistic [6, 7] mean-field (MF) theory, Hartree-Fock (HF) model with the pairing correlations of Bardeen, Cooper and Schrieffer BCS [8], relativistic and nonrelativistic random phase approximation (RPA) [9–11].

It is possible to get insight into the microscopic structure and collective behavior of giant resonances GR through experimental studies of their direct decay modes. Theoretically, transition amplitudes of RPA can be used to explain the GR. This GR depends on nuclei characteristics, such as the number of nucleons involved in the response and the size of the nucleus [12].

By determining the resonance energies of the isoscalar giant monopole resonance (ISGMR) and the isoscalar giant dipole resonance (ISGDR), researchers are primarily interested in investigating nuclear incompressibility [13–16]. The incompressibility is a key factor when using the nuclear

equation-of-state to simulate computations for different astrophysical events or to describe heavy-ion reactions.

The isoscalar giant quadrupole resonance (ISGQR) was found in the early 1970s [17–19], and the isoscalar giant monopole resonance (ISGMR) was reported in 1977 [20, 21]. Throughout the 1980s, the ISGMR was the focus of numerous investigations [22–24]. The isoscalar giant dipole resonance (ISGDR) in ^{208}Pb was initially described by Morsch et al. [25], but Davis et al. [26] provided a definitive identification. ISGMR and ISGDR are both considered compression modes and offer details regarding nuclear incompressibility, K_A.

Several theoretical [9–11, 15], and experimental [27, 28] publications have been published that detail the findings of investigations into the characteristics of the isoscalar dipole resonance in a number of medium-heavy mass spherical nuclei. It was discovered by Clark et al. [28] that the isoscalar dipole strength distribution exhibits two main peaks of strength concentration, which correspond to the lower PDR and higher GDR components. The RPA calculations provide significant support for the PDR, which depicts the extra neutrons at the nuclear surface (neutron skin) vibrating against the nucleus's core. Studies of compression modes of nuclei are of particular interest since their strength distributions $S(E)$ are sensitive to the value of the nuclear matter incompressibility coefficient K [14], [29], [30].

There are 33 known isotopes of molybdenum (Z=42), with atomic masses ranging from 83 to 115, as well as four metastable nuclear isomers. Seven isotopes having atomic masses of 92, 94, 95, 96, 97, 98, and 100 are found in nature. Molybdenum's unstable isotopes all undergo isotopic decay to form ruthenium, technetium, zirconium, and niobium. The sole unstable naturally occurring isotope is ^{100}Mo, which has a half-life of about 1×10^{19} years and double beta decays into ^{100}Ru [31].

Moalem et al. were the first to notice isoscalar giant resonances in the Mo isotopes, and they used inelastic scattering of 110 MeV 3He to pinpoint the Giant Quadrupole Resonance (GQR) in all stable

Mo isotopes [32]. The GQR and GMR in ^{92}Mo were examined by Duhamel et al. [33] using inelastic scattering of 152 MeV particles. Youngblood et al. used inelastic scattering of 240 MeV particles at small angles, including 0°, to investigate the isoscalar giant resonances in ^{90,92,94}Zr and ^{92,96,98,100}Mo [34–36]. According to Youngblood et al. [34], the E0 strength distribution of these Zr and Mo isotopes revealed high and low-energy components separated by 7-9 MeV. The HF-RPA calculations, which replicate the ISGMR energies in the other nuclei, do not predict the higher energy second peak.

The excellent peak to continuum ratio [37–40] of data obtained with 240 MeV α particles allows the identification of the GDR, GQR, and High Energy Octupole Resonance (HEOR) strength distributions in the range $9 \leq Ex \leq 36$ MeV. The strength distributions for these resonances in Mo [35] isotopes were investigated and compared to the results of spherical HF based on HF-RPA calculations [41] with KDE0v1 Skyrme-type effective interaction [42].

In this work, we employ the self-consistent Skyrme QRPA approach on top of HF-BCS, to study the isoscalar (IS) Giant Dipole Resonance (GDR) and Pygme Dipole Resonance (PDR) in ^{92}Mo and ^{100}Mo isotopes. The HF-BCS equations are first solved in coordinate space using a radial mesh that reaches up to 200 fm (with a step of 0.1 fm). The HF equations contain the Skyrme NN interaction, and in this work, we have selected 10 Skyrme parameter sets: KDE0v1 [42], eMSL08 [43], SKX [44], SGOI [45], v080 [46], SKP [47], SIV [48], SIII [49], SKIII [50], and SGI [45] of different values for the nuclear matter incompressibility K_{NM} = 200.8, 227.54, 229, 231.117, 269, 271.06, 300, 324.55, 356, and 361.59 MeV, respectively. Having a large number of Skyrme-force parameterizations requires a continuous search for the best for describing the experimental data. To establish the best sets of Skyrme-force parameterizations for defining the experimental data, the strength function and centroid energy of the isoscalar ISGDR (J^{π}; T = 1^{-}; 0) were compared with the available experimental data. It was also studied how the computed centroid energy changes with values of K_{NM} and A. This research trend is

crucial for creating a successful theoretical model that is in good agreement with experimental data.

Formalism

Both spherical and deformed nuclei's ground-state properties are extremely well described by the density-dependent HF+BCS approximation [51, 52], where the variational approach can be applied to an ansatz φ (trial wave function) that is a product of single-particle functions to determine the total energy E of HF equations based on Skyrme-type interaction [52, 53],

$$\langle \delta\varphi | H(r) | \varphi \rangle = 0 \tag{1}$$

The total HF-BCS energy can be calculated directly from the force, or energy functional,

$$E = E_{KE} + E_{Skyrme} + E_{Coul} + E_{pair} \tag{2}$$

Where E_{KE}, E_{Skyrme}, E_{Coul} , and E_{Pair} are the Kinetic, Skyrme, Coulomb and Pair contributions to the energy. E_{KE} and E_{Skyrme} equations given by Chabanat et al. and Ryssens et al. [54, 55]. The E_{Coul} has a direct part and an exchange part that is calculated in the usual Slater approximation. The E_{Pair} can be found in [55].

On top of the HF+BCS ground state, the excited states are calculated within the QRPA model. The compact form of QRPA equations can be written as follows [56, 57],

$$\begin{pmatrix} A_{ab,cd} & B_{ab,cd} \\ -B^*_{ab,cd} & -A^*_{ab,cd} \end{pmatrix} \begin{pmatrix} X^{\upsilon}_{cd} \\ Y^{\upsilon}_{cd} \end{pmatrix} = \hbar\Omega_{\upsilon} \begin{pmatrix} X^{\upsilon}_{ab} \\ Y^{\upsilon}_{ab} \end{pmatrix}, \tag{3}$$

where $X^{\upsilon}_{\square}$ and $Y^{\upsilon}_{\square}$ are the eigenvectors (amplitudes) and $\hbar\Omega_{\upsilon}$ is the eigenvalue (excited energy) of the υ^{th} state. On the HF-BCS two-quasiparticle basis, the sub-matrices A and B take the form

$$\begin{aligned} A_{ab,cd} = (1+\delta_{ab})^{-\frac{1}{2}} (1+\delta_{cd})^{-\frac{1}{2}} \big[& (E_{a+E_b})\, \delta_{ac}\delta_{bd} \\ & + (u_a u_b u_c u_d + v_a v_b v_c v_d)\, G\,(abcd;J) \\ & + (u_a v_b u_c v_d + v_a u_b v_c u_d)\, F\,(abcd;J) \\ & - (-1)^{j_c + j_d - J'} (u_a v_b v_c u_d + v_a u_b u_c v_d) F(abcd;J) \Big], \end{aligned} \tag{4}$$

$$B_{ab,cd} = (1+\delta_{ab})^{-\frac{1}{2}}(1+\delta_{cd})^{-\frac{1}{2}}\left[-(u_a u_b v_c v_d + v_a v_b u_c u_d)\,G(abcd;J)\right.$$
$$-(-1)^{j_c+j_d-J'}(u_a v_b u_c v_d + v_a u_b v_c u_d)F(abcd;J)$$
$$\left.+(-1)^{j_a+j_b+j_c+j_d-J-J'}(u_a v_b v_c u_d + v_a u_b u_c v_d)F(abcd;J)\right], \quad (5)$$

with,

$$G(abcd;J) = \sum_{m_a m_b m_c m_d} \langle j_a m_a j_b m_b | JM\rangle \langle j_c m_c j_d m_d | J'M'\rangle V^{pp}_{ab,cd}, \quad (6)$$

$$F(abcd;J) = \sum_{m_a m_b m_c m_d} \langle j_a m_a j_b m_b | JM\rangle \langle j_c m_c j_d m_d | J'M'\rangle V^{ph}_{ab,cd}. \quad (7)$$

$V^{pp}_{ab,cd}$ and $V^{ph}_{ab,cd}$ are matrix elements of particle-particle (pp) and particle-hole (ph) effective interaction, respectively. The Pandya transformation of ph matrix elements is defined as [58–60],

$$V^{ph}_{ab,cd} = -\sum_{J'}(2J'+1)\begin{Bmatrix} J_a & J_d & J' \\ J_c & J_b & J \end{Bmatrix} V^{pp}_{ad,cb} \quad (8)$$

After solving the QRPA equations, various moments of the strength distributions can be obtained by means of the following equation [61],

$$m_k = \int E^k S(E)\, dE \quad (9)$$

where $S(E)$ is the strength function [62],

$$S(E) = \sum_v |\langle v|\hat{F}_J|0\rangle|^2 \rho_\Gamma(E - E_v) \quad (10)$$

associated with the monopole operator where the Lorentzian function is defined as in the following,

$$\rho_\Gamma(E - E_v) = \frac{\Gamma}{2\Pi}\frac{1}{(E-E_v)^2 + \left(\frac{\Gamma}{2}\right)^2} \quad (11)$$

with Γ is the smearing parameter.

In this work, the Pearson linear correlation coefficient has been calculated in order to study the sensitivity of the E_{cen} to the values of Nuclear Matter (NM) properties associated with the Skyrme force according to the following equation

$$C = \frac{\Sigma_{i=1}^{n} (x_i - \overline{x})(y_i - \overline{y})}{\sqrt{\sum_{i=1}^{n} (x_i - \overline{x})^2} \sqrt{\sum_{i=1}^{n} (y_i - \overline{y})^2}} \tag{12}$$

where $\overline{x}$ ($\overline{y}$) are the averages of the two quantities $x(y)$.

Results and Discussion

In order to investigate the IS GDR and PDR of the ^{92,100}Mo isotopes, the static HF+BCS equations were solved by the Numerov method using a radial mesh size of 0.1 fm in a model space based on ten Skyrme interaction sets, namely KDE0v1 [42], eMSL08 [43], SKX [44] , SGOI [45], v080 [46], SKP [47], SIV[48], SIII [49], SKIII [50], and SGI [45] then the QRPA matrix diagonalization have been performed in the selected model space.

To comprehend the structural and bulk properties of nuclear systems, it is crucial to grasp the collective modes in nuclei. Our calculated of the strength function for the ^{92,100}Mo isotopes (shown in Fig. 1 as fraction EWSR/MeV) have been done in the long wavelength limit for the low-lying IS GDR and PDR with smearing parameter Γ=3 and 5 MeV, and compared with the experimental data [35, 63]. The general behavior of the experimental strength distribution is well described for most of the interactions, especially with Γ=3 MeV. Our calculated centroid energy E_{cen}, scaled energies E_s and constrained energy E_{con} are presented in Table 1 in comparison with the available data.

For ^{92}Mo, the fraction EWSR/MeV of ISPDR of in the range E_x=9-20 MeV (with m_1/m_0 ∼10 MeV for SGI, m_1/m_0 ∼13.5 MeV for SKP, SIV, SKIII, m_1/m_0 ∼15 MeV for SKX, SGOI, v080 and SIII, while the ISGDR in the range E_x=20-40 MeV with m_1/m_0 ∼25.5 MeV for KDE0v1, eMSL08 and v080, for SKX, SGOI, SGI, SIII and SIV, the $m_1/m_0 \sim$ 27, 29, 27, 29, 34 MeV respectively,

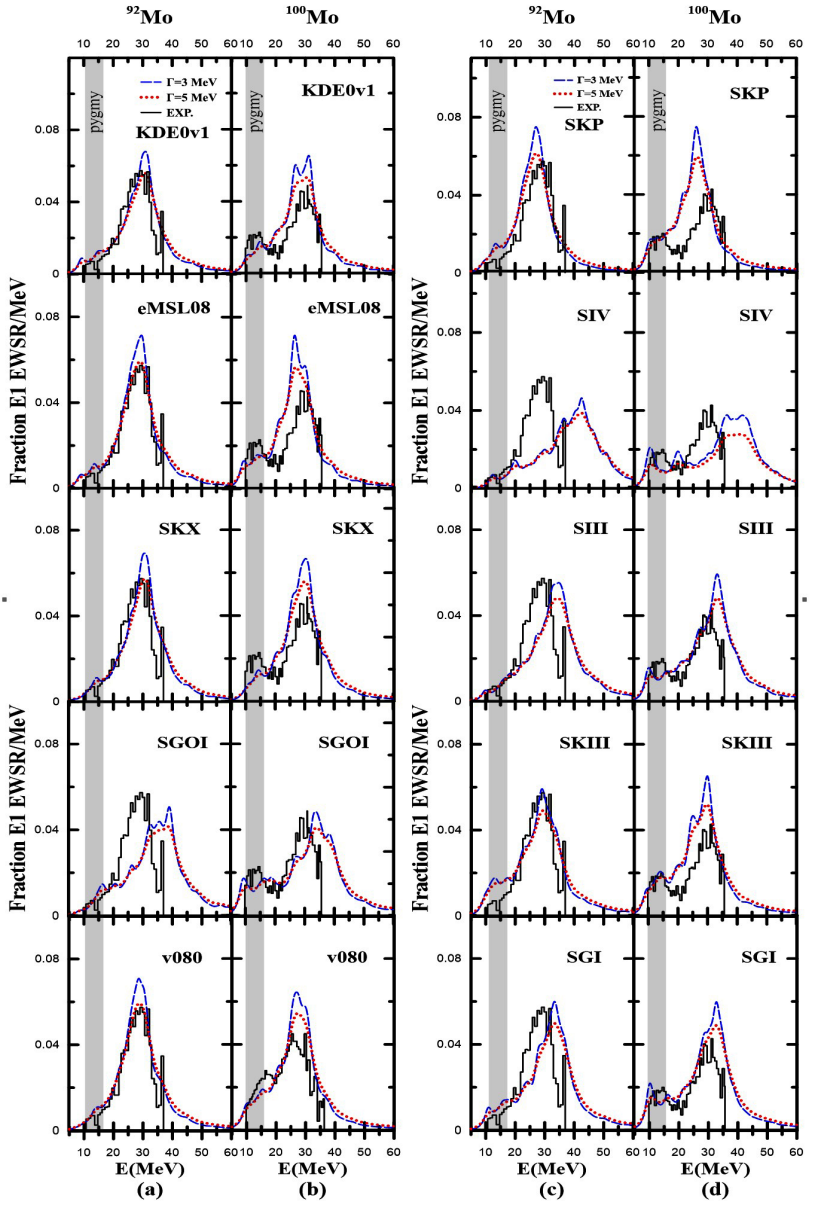

FIGURE 1. *Our calculated fraction EWSR/MeV of ISGDR E1 for (a and c) ^{92}Mo, (b and d) ^{100}Mo, using self-consistent HFBCS+QRPA with Skyrme interactions: KDE0v1, eMSL08, SKX, SGOI, v080, SKP, SIV, SIII, SKIII, and SGI compared with the experimental data [35] (black-solid lines). Blue dashed lines and red dotted lines both have smearing widths of 3 and 5 MeV, respectively.*

m_1/m_0 ∼23.5 for SKIII and SKP, whereas the data peak around ∼28 MeV.

	$E_{cen} = \left(\frac{m_1}{m_0}\right)$		$E_s = \sqrt{\left(\frac{m_3}{m_1}\right)}$		$E_{con} = \sqrt{\left(\frac{m_1}{m_{-1}}\right)}$	
Isotopes	^{92}Mo	^{100}Mo	^{92}Mo	^{100}Mo	^{92}Mo	^{100}Mo
Exp.	27.6 ± 0.5	30.1±0.7	.....	.....	.....	.....
SKP	23.6	21.363	26.674	25.079	22.278	19.806
KDE0v1	25.404	24.42	29.788	28.303	23.242	22.716
eMSL08	24.943	22.57	28.626	26.798	23.11	20.572
v080	26.029	22.89	29.013	26.829	24.831	21.192
SGI	27.151	23.659	32.056	29.737	24.929	21.005
SKX	27.275	25.369	30.704	29.057	25.86	23.743
SKIII	23.921	22.699	28.713	27.561	21.951	20.675
SIV	33.985	26.668	40.444	36.808	31.083	22.493
SIII	29.092	25.055	33.76	31.272	26.878	22.216
SGOI	29.847	24.325	35.301	32.266	27,383	20.939

TABLE 1. *Our calculated E_{cen}, E_s and E_{con} for ISGDR in $^{92,100}Mo$ are compared with experimental data [35].*

For ^{100}Mo the fraction EWSR/MeV of ISPDR in the range E_x=9-20 MeV with m_1/m_0 ∼15 MeV for KDE0v1, eSML08, SKX, v080, SKIII and m_1/m_0 ∼10 for SGOI, SKP, SIV, SIII, and SGI, while ISGDR in the range E_x=20-40 MeV with m_1/m_0 ∼24 MeV for KDE0v1 and SGOI. For the high energy component is between 21-27 MeV for all other types of Skyrme force, whereas the data peak around ∼30 MeV and are substantially lower than the calculation in the 28 MeV region.

In Figure 2, the centroids of the strength in the high peaks (GDR) for the isotopes from Ref. [35] and for ^{92,100}Mo is plotted vs. A for the ^{100}Mo isotope, for the majority of the used sets of Skyrme interaction, the estimated positions of the high energy peaks frequently diverge from the experimental position, where the strength seen experimentally is somewhat less than predicted to

lie in this energy range. The SKX and SGI are agreement strongly with the experimental position for ^{92}Mo, where the E_{cen} for SKX and SGI is corresponded with the experimental data.

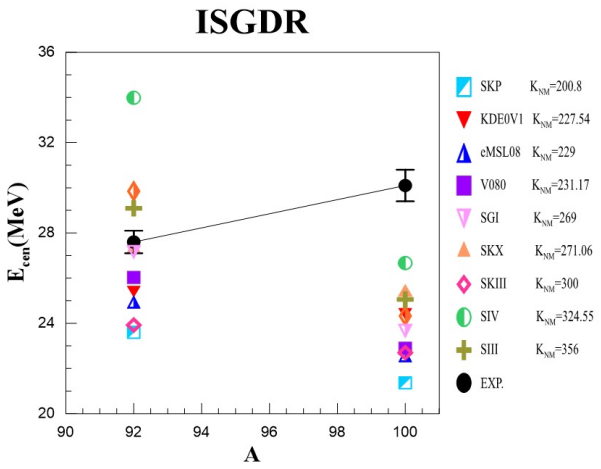

FIGURE 2. *(Color online) Our calculated E_{cen} vs. A of the ISGDR for the investigated Mo isotopes in comparison with experimental values (black) [35].*

Figure 3 shows our calculated fraction EWSR/MeV of ISGDR for ^{92}Mo and ^{100}Mo, using 10 types of Skyrme interactions of different nuclear matter incompressibility K_{NM} with Γ=3 MeV compared with the experimental data [35] (black-solid lines). It appears that the type of interaction has a clear effect on the strength distribution of ISGDR. In ISGDR, a high K_{NM} causes the peak to shift to a higher energy while a low K_{NM} causes the peak to shift to a lower energy. For example, an SGOI interaction with a high K_{NM} of 361.59 MeV causes the centroid energy to be 29.847 MeV for ^{92}Mo and 24.325 MeV for ^{100}Mo and a low K_{NM} of 200.8 MeV causes the centroid energy to be 23.6 MeV and 21.363 MeV for ^{92}Mo and ^{100}Mo. The experimental value of m_1/m_0 =27.6±0.5 MeV and 30.1±0.7 MeV [36] for ^{92}Mo and ^{100}Mo as shown in Table 1. Fig.3 shows the significant change in the strength distribution with changing values of K_{NM}.

For the low energy PDR, the strength distributions are concentrated in a single peak around 15 MeV and for the high

energy dipole resonance, the strength distributions are concentrated in a single peak around ∼29 MeV. However, the location of the peak found with each Skyrme interaction is slightly different. The SkP interaction predicts lowest peaks while the SGOI interaction gives peaks at the highest energies. As it is known from previous studies, the relative position of the peaks is governed by the nuclear matter incompressibility associated with each effective interaction.

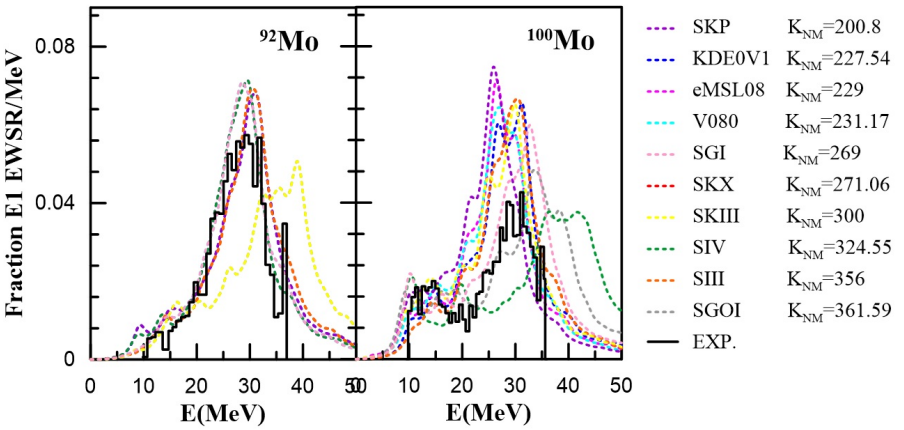

FIGURE 3. *Our calculated fraction EWSR/MeV of ISGDR for ^{92}Mo and ^{100}Mo, using 10 types of Skyrme interactions (with their nuclear matter incompressibility K_{NM}) with* Γ*=3 MeV compared with the experimental data [35] (black-solid lines).*

The calculated centroid energies, E_{cen} of the ISGDR of ^{92,100}Mo isotopes are plotted against the K_{NM} incompressibility coefficient in Fig. 4. The experimental region is delimited by the dashed lines. We found a medium correlation between K_{NM} and the centroid energy with Pearson linear correlation coefficients C ∼ 0.709 and 0.625 for ^{92}Mo and ^{100}Mo, respectively, where the correlation coefficients were calculated using the Eq. (12). Pearson correlation coefficient, also known as Pearson statistical test, measures the strength between the different variables (K_{NM}, E_{cen}) and their relationships. Therefore, whenever any statistical test is conducted between them, it is always a good idea for the person analyzing to calculate the value of the correlation coefficient to know how strong the relationship between the two variables is.

Pearson's correlation coefficient can range from the value +1 to the value -1, where +1 indicates the perfect positive relationship between the variables, -1 indicates the perfect negative relationship between the variables, and 0 value indicates that no relationship exists between the variables.

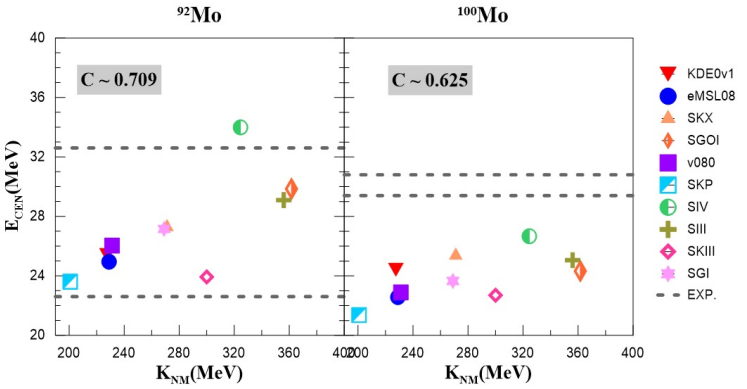

FIGURE 4. *Our obtained E_{cen} of ISGDR for $^{92,100}Mo$ vs. K_{NM} in comparison with the experimental region is delimited by the dashed lines [35].*

Conclusions

A significant description of the collective low-lying ISGDR and ISPDR with $\Gamma = 3$ MeV is provided by the self-consistent HFBCS+QRPA calculations with Skyrme interactions. The peak high, widths, and (smooth) profiles of strength of the examined ^{92}Mo isotope with SKX, SGI agree with the data. The E_{cen} values that are in agreement with experimental data are those that drop as A increases and those that use interactions of K_{NM} between 269 and 271 MeV. Medium correlation between K_{NM} and the centroid energy were obtained with Pearson linear correlation coefficients C ∼0.709 and 0.625 for ^{92}Mo and ^{100}Mo, respectively.

References

[1] E. Caurier, P. Navrátil, W. E. Ormand, and J. P. Vary, Phys. Rev. C **66**, 024314 (2002).

[2] S. Beane and e. a. Chang, Phys. Rev. Lett. **115**, 132001 (2015).
[3] S. Koonin, D. Dean, and K. Langanke, Phys. Rep. **278**, 1 (1997).
[4] T. Otsuka, Nucl. Phys. A **693**, 383 (2001).
[5] P. Reinhard, Rep. Prog. Phys. **52**, 439 (1989).
[6] J. Dobaczewski, W. Nazarewicz, T. R. Werner, J. F. Berger, C. R. Chinn, and J. Dechargé, Phys. Rev. C **53**, 2809 (1996).
[7] J. Dobaczewski, M. Stoitsov, and W. Nazarewicz, AIP Conf. Proc. **726**, 51 (2004).
[8] T. Werner, J. Sheikh, W. Nazarewicz, M. Strayer, and A. Umar, Phys. Lett. B **335**, 259 (1994).
[9] M. L. Gorelik, S. Shlomo, and M. H. Urin, Phys. Rev. C **62**, 044301 (2000).
[10] D. Vretenar, A. Wandelt, and P. Ring, Phys. Lett. B **487**, 334 (2000).
[11] S. Shlomo and A. Sanzhur, Phys. Rev. C **65**, 044310 (2002).
[12] M. Harakeh and A. van der Woude, *Giant Resonances: Fundamental High-Frequency Modes of Nuclear Excitations* (Oxford St. in Nucl Phys., 2001).
[13] M. Harakeh and A. Dieperink, Phys. Rev. C **23**, 2329 (1981).
[14] S. Stringari, Phys. Lett. B **108**, 232 (1982).
[15] G. Colò, N. Van Giai, P. Bortignon, and M. Quaglia, Phys. Lett. B **485**, 362 (2000).
[16] S. Shlomo and A. Sanzhur, Phys. Rev. C **65**, 044310 (2002).
[17] R. Pitthan and T. Walcher, Phys. Lett. B **36**, 563 (1971).
[18] S. Fukuda and Y. Torizuka, Phys. Rev. Lett. **29**, 1109 (1972).
[19] M. Lewis and F. Bertrand, Nucl. Phys. A **196**, 337 (1972).
[20] M. Harakeh, K. van der Borg, T. Ishimatsu, H. Morsch, A. van der Woude, and F. Bertrand, Phys. Rev. Lett. **38**, 676 (1977).
[21] D. Youngblood, C. Rozsa, J. Moss, D. Brown, and J. Bronson, Phys. Rev. Lett. **39**, 1188 (1977).
[22] A. van der Woude and J. Speth, *The electric giant resonances.*, Vol. 24 (Singapore: World Scientific, 1991).

[23] D. H. Youngblood, P. Bogucki, J. D. Bronson, U. Garg, Y. W. Lui, and C. M. Rozsa, Phys. Rev. C **23**, 1997 (1981).

[24] M. M. Sharma, W. T. A. Borghols, S. Brandenburg, S. Crona, A. van der Woude, and M. N. Harakeh, Phys. Rev. C **38**, 2562 (1988).

[25] H. P. Morsch, M. Rogge, P. Turek, and C. Mayer-Böricke, Phys. Rev. Lett. **45**, 337 (1980).

[26] B. F. Davis, U. Garg, W. Reviol, M. N. Harakeh, A. Bacher, G. P. A. Berg, C. C. Foster, E. J. Stephenson, Y. Wang, J. Jänecke, K. Pham, D. Roberts, H. Akimune, M. Fujiwara, and J. Lisantti, Phys. Rev. Lett. **79**, 609 (1997).

[27] H. Clark, Y.-W. Lui, D. Youngblood, K. Bachtr, U. Garg, M. Harakeh, and N. Kalantar-Nayestanaki, Nuc. Phys. A **649**, 57 (1999).

[28] H. L. Clark, Y.-W. Lui, and D. H. Youngblood, Phys. Rev. C **63**, 031301 (2001).

[29] A. Bohr and B. Mottelson, *Nuclear Structure, Volume II: Nuclear Deformations*, Vol. II (W. A. Benjamin, 1975).

[30] S. Shlomo and D. H. Youngblood, Phys. Rev. C **47**, 529 (1993).

[31] D. R. Lide, J. Am. Chem. Soc. **129**, 724 (2007).

[32] A. Moalem, Y. Gaillard, A. Bemolle, M. Buenerd, J. Chauvin, G. Duhamel, D. Lebrun, P. Martin, G. Perrin, and P. de Saintignon, Phys. Rev. C **20**, 1593 (1979).

[33] G. Duhamel, M. Buenerd, P. de Saintignon, J. Chauvin, D. Lebrun, P. Martin, and G. Perrin, Phys. Rev. C Nucl. Phys. **38**, 2509 (1988).

[34] D. H. Youngblood, Y. Lui, Krishichayan, J. Button, M. R. Anders, M. L. Gorelik, M. H. Urin, and S. Shlomo, Phys. Rev. C **88**, 021301 (2013).

[35] D. H. Youngblood, Y.-W. Lui, Krishichayan, J. Button, G. Bonasera, and S. Shlomo, Phys. Rev. C **92**, 014318 (2015).

[36] Krishichayan, Y. Lui, J. Button, D. H. Youngblood, G. Bonasera, and S. Shlomo, Phys. Rev. C **92**, 044323 (2015).

[37] D. H. Youngblood, Y.-W. Lui, and H. L. Clark, Phys. Rev. C **65**, 034302 (2002).

[38] D. H. Youngblood, Y.-W. Lui, and H. L. Clark, Phys. Rev. C **63**, 067301 (2001).

[39] Y.-W. Lui, H. L. Clark, and D. H. Youngblood, Phys. Rev. C **61**, 067307 (2000).

[40] D. H. Youngblood, Y.-W. Lui, and H. L. Clark, Phys. Rev. C **60**, 014304 (1999).

[41] P.-G. Reinhard, Ann. Phys. **504**, 632 (1992).

[42] B. K. Agrawal, S. Shlomo, and V. Kim Au, Phys. Rev. C **72**, 014310 (2005).

[43] Z. Zhang and L.-W. Chen, Phys. Rev. C **94**, 064326 (2016).

[44] B. Alex Brown, Phys. Rev. C **58**, 220 (1998).

[45] Q.-B. Shen, Y.-L. Han, and H.-R. Guo, Phys. Rev. C **80**, 024604 (2009).

[46] J. M. Pearson and S. Goriely, Phys. Rev. C **64**, 027301 (2001).

[47] P.-G. Reinhard, D. J. Dean, W. Nazarewicz, J. Dobaczewski, J. A. Maruhn, and M. R. Strayer, Phys. Rev. C **60**, 014316 (1999).

[48] B. A. Brown, G. Shen, G. C. Hillhouse, J. Meng, and A. Trzcińska, Phys. Rev. C **76**, 034305 (2007).

[49] H. Köhler, Nucl. Phy. A **258**, 301 (1976).

[50] S. Krewald, V. Klemt, J. Speth, and A. Faessler, Nucl. Phy. A **281**, 166 (1977).

[51] P. Bonche, H. Flocard, P. Heenen, S. Krieger, and M. Weiss, Nucl. Phy. A **443**, 39 (1985).

[52] M. Bender, P.-H. Heenen, and P.-G. Reinhard, Rev. Mod. Phys. **75**, 121 (2003).

[53] D. Vautherin and D. M. Brink, Phys. Rev. C **5**, 626 (1972).

[54] E. Chabanat, P. Bonche, P. Haensel, J. Meyer, and R. Schaeffer, Nucl. Phys. A **635**, 231 (1998).

[55] W. Ryssens, V. Hellemans, M. Bender, and P.-H. Heenen, Comp. Phys. Commun. **187**, 175 (2015).

[56] D. Rowe, *Nuclear Collective Motion: Models and Theory* (World Scientific, 2010).

[57] P. Ring and P. Schuck, *The Nuclear Many Body Problem*

(Springer, 1980).

[58] G. Colò, L. Cao, N. Van Giai, and L. Capelli, Comp. Phys. Commun. **184**, 142 (2013).

[59] A. H. Taqi and G. L. Alawi, Nucl. Phys. A **983**, 103 (2019).

[60] A. H. Taqi and G. L. Alawi, Nucl. Phys. At. Energy **19**, 326 (2018).

[61] S. Amin, A. A. Al-Rubaiee, and A. Taqi, KUJSS **17**, 17 (2022).

[62] A. Taqi and M. S. Ali, Indian J.Phys. **92**, 69 (2018).

[63] J. Button, Y. Lui, D. Youngblood, X. Chen, G. Bonasera, and S. Shlomo, Phys. Rev. C **94**, 034315 (2016).